designs

MDPI

Article

Evaluation of the Compressive Strength of CFRP-Wrapped Circular Concrete Columns Using Artificial Intelligence Techniques

Kennedy C. Onyelowe [1], Jagan Jayabalan [2], Ahmed M. Ebid [3,*], Pijush Samui [4], Rahul Pratap Singh [5], Atefeh Soleymani [6] and Hashem Jahangir [7]

1 Department of Civil Engineering, Michael Okpara University of Agriculture, Umudike 440101, Nigeria
2 Department of Civil Engineering, Galgotias University, Greater Noida 203201, Uttar Pradesh, India
3 Department of Structural Engineering, Future University in Egypt, New Cairo 11865, Egypt
4 Department of Civil Engineering, National Institute of Technology, Patna 800005, Bihar, India
5 Department of Civil Engineering, National Institute of Technology, Kurukshetra 136119, Haryana, India
6 Department of Structural Engineering, Shahid Bahonar University of Kerman, Kerman 76169-14111, Iran
7 Department of Civil Engineering, University of Birjand, Birjand 97174-31349, Iran
* Correspondence: ahmed.abdelkhaleq@fue.edu.eg

Abstract: The wrapping of concrete structures with fiber polymers has been an essential part of concrete technology aimed at the improvement of concrete performance indices during the construction and lifelong usage of the structures. In this paper, a universal representative database was collected from multiple literature materials on the effect of different fiber-reinforced polymers on the confined compressive strength of wrapped concrete columns (Fcc). The collected data show that the Fcc value depends on the FRP thickness (t), tensile strength (Ftf), and elastic modulus (Ef), in addition to the column diameter (d) and the confined compressive strength of concrete (Fco). Five AI techniques were applied on the collected database, namely genetic programming (GP), three artificial neural networks (ANN) trained using three different algorithms, "back Propagation BP, gradually reduced gradient GRG and genetic algorithm GA", and evolutionary polynomial regression (EPR). The results of the five developed predictive models show that (t) and Ftf have a major impact on the Fcc value, which presents the effect of confinement stress (t. Ftf/d) on the confined compressive strength (Fcc). Comparing the predicted values with the experimental ones showed that the GP model is the least accurate one, and the EPR model is the next least accurate, while the three ANN models have almost the same level of high accuracy, with an average error percentage of 5.8% and a coefficient of determination R^2 of 0.961. The ANN model is more accurate than the EPR and GP predictive models, but they are suitable for manual calculation because they are closed-form equations.

Keywords: CFRP-wrapped concrete; circular RC column; AI techniques; axial compression capacity

Citation: Onyelowe, K.C.; Jayabalan, J.; Ebid, A.M.; Samui, P.; Singh, R.P.; Soleymani, A.; Jahangir, H. Evaluation of the Compressive Strength of CFRP-Wrapped Circular Concrete Columns Using Artificial Intelligence Techniques. *Designs* **2022**, *6*, 112. https://doi.org/10.3390/designs6060112

Academic Editor: Eric M. Lui

Received: 8 October 2022
Accepted: 2 November 2022
Published: 9 November 2022

1. Introduction

Many RC buildings, particularly in developing nations, need to be strengthened. The demolition of old buildings and manufacture of new buildings is an expensive and time-demanding procedure [1]. Some of the reasons for using strengthening techniques are the age of the structure and damage from natural corrosive agents, seismic events, and environmental disasters [2–6].

Exterior confining by using carbon fiber-reinforced polymers (CFRPs) is among the most prevalent approaches for strengthening RC columns and expanding capacity. CFRP has a number of advantages over other typical engineering materials, including excellent confining ability when wrapped, high strength and stiffness, high durability, chemical resistance, tunable thermal characteristics, non-magnetic nature, and lighter weight. It also improves the columns' seismic performance [7–14]. The excellent tensile strength of CFRP

can tightly confine the columns; the lateral confining force compresses the concrete in three axes, improving the compressive strength of the concrete [13].

The kind of CFRP, material modulus and strength, CFRP thickness, number of CFRP layers, fiber orientation, and CFRP execution technique all have an influence on the structural performance of RC columns [15]. The simplicity with which CFRP sheets may be fitted has sped up the retrofitting process, and their low cost and lightweight nature have enhanced their appeal [16–19]. Surface embedding systems that use near-surface mount (NSM) bars or strips glued to grooves cut into the concrete surface based on the reinforcement mechanism can be divided into two categories: externally bonded (EB) surface tools with plates or sheets, and surface-embedded applications with near-surface-mounted (NSM) bars or strips bonded into furrows cut into the concrete surface [20]. Wrapping RC columns with CFRP sheets has lately become more popular as a method of retrofitting. This retrofitting method not only prevents the longitudinal reinforcement of the column from buckling, but also slows the column's collapse by postponing the concrete cover's spalling [21,22]. The utilization of CFRP sheets to retrofit structural RC elements, especially in earthquake regions, has proven to be successful [15,23]. Using CFRP sheets improves the strength, ductility, and stiffness of RC columns by increasing the concrete core's confinement. Covering RC columns with CFRP jackets is beneficial in a variety of building projects.

Using CFRP to confine concrete has been the subject of numerous investigations. The CFRP jacket's confinement effectiveness for a rectangular section is determined by various factors, including the CFRP's stiffness and volumetric ratio, the aspect ratio of the section, and the concrete section's corner radius [24–26]. Many studies [24,27–31] have examined the behavior of undamaged concrete columns encased in CFRP jackets under concentric and eccentric stresses; for example, Parvin and Wang [32] used nine small sizes (108 × 108 × 305 mm) to be precise. Low-eccentricity loads (eccentricity ratios (e/h) of 0, 0.07, and 0.14) were applied to concrete columns confined using zero, one, and two layers of unidirectional CFRP. The ultimate loads of the columns were attained when the fibers experienced hoop rupture. Furthermore, the confinement effect diminished as eccentricity grew. The application of CFRP sheets to reinforce and increase the column's flexural capacity when exposed to flexure and compression was suggested by Barros et al. [33]. Fitzwilliam and Bisby [34] investigated the load-bearing capability of RC circular columns confined by CFRP when subjected to eccentric axial compression. The use of CFRP hoop warps boosted the strength and deformation resistance capacity of both short and slender columns, according to the findings. The CFRP strips offered extra confinement, which enhanced the column's bearing capacity by 28.5 percent and postponed local buckling. Hadi and Le [35] examined the impact of fiber orientation in sheets of CFRP (at 0°, 45°, and 90° angles) on the performance of concentrically and eccentrically loaded hollow-core square-section RC columns covered with CFRP. They noticed that retrofitting the hollow-core square-section columns increased their performance. In addition, when wrapped in solely hoop-oriented layers, the columns' ductility and strength were greatly enhanced. CFRP sheets that were bidirectional improved confining effectiveness, ductility, and ultimate strength capacity in slender RC columns, according to Dundar et al. [15], and using more CFRP sheet layers enhanced confining effectiveness and load-bearing capacity, according to Dundar et al. (by approximately 20 percent and 40 percent for one- and two-layer confinement, respectively). Furthermore, concrete's compressive strength and the eccentricity of the load and of RC columns' slenderness when wrapped by CFRP sheets was found to have a substantial impact on the columns' behavior. In a recent study by Chellapandian et al. [36], it was found that a hybrid confining approach including NSM composite materials and CFRP sheets was more effective in enhancing the strength and ductility of RC columns under compression stress than either the NSM system or the CFRP jacket alone. Cao et al. [37] studied the performance of non-reinforced concrete encased in CFRP when subjected to eccentric stress, and it was discovered that growth in the number of CFRP sheets enhanced the ultimate load capacity. The findings of Nematzadeh

et al. [19] showed that the CFRP jacket improved the load-bearing capacity and ductility of RC columns, but the use of steel fibers in the concrete had no influence on the columns' loading capacity; however, their ductility increased. Furthermore, the eccentric applied force minimized the impact of CFRP sheet confinement on RC strength [38–43]. Deng et al. [13] demonstrated a CFRP-confined coral aggregate concrete (CAC) column. As a one-of-a-kind composite column suitable for use in marine circumstances, according to test results, the CFRP jacket greatly increased the load-bearing capacity and ductility of the CAC stub columns [24,44–46]. This paper aims to develop a global predictive model for the axial compressive strength of short round concrete columns, which, in previous research works on this subject, were not considered, and more so the application of multiple intelligent models. Fathi et al. [47] used the artificial neural network (ANN) to formulate the compressive strength (Fcc) of CFRP-confined concrete cylinders and also achieved satisfactory accuracy when compared to experimental values. Conversely, the support vector machine (SVM) was applied by Aires Camoes and Francisco Ferreira Martins in the prediction of the compressive strength of concrete cylinders confined with CFRP, also taking into account the specimen's circular cross-section. The models developed must be valid for any type of FRP, and, therefore, the characteristics of FRP that express the type of FRP used, such as tensile strength (Ftf) and the modulus of elasticity (Ef), was considered in the present work. The properties of FRP mainly depend on the fibers–epoxy ratio, which in itself depends on the experience and efficiency of the labor used, which causes a large variation in FRP properties and, accordingly, in the confined compressive strength of concrete. In order to deal with these large and random variations, artificial intelligence techniques were the most suitable techniques to develop the predictive model. Moreover, this research is important because, with the proposed models for the compressive strength of CFRP-confined concrete columns with circular cross-sections, repeated visits to the laboratory to investigate the design and behavior of such structural members are reduced. The following section describes the methodology used to develop the model.

The domain of civil engineering is becoming increasingly influenced by machine learning approaches. Concrete's mechanical properties can be forecasted by using these approaches extensively. An extensive amount of data is used to build a precise model using these techniques. Experimental work or literature study accuracy depends on the data sample used or the specimen cast [48]. It is impossible to determine exact coefficients for these models, since concrete properties and controlling factors are highly non-linear. Researchers, therefore, are employing machine learning (ML) applications to predict concrete qualities [48].

Machine learning (ML) methods can be used to estimate concrete's compressive strength thanks to the recent evolution of artificial intelligence. Clustering, classification, and regression, among others, can be achieved using the ML approach. A regression function in machine learning can be used to estimate concrete's compressive loading capacity. The results given by ML are far more accurate than those of the previous regression methods [49].

Two distinct techniques were presented in a paper by Perera et al. [50]. Initially, neural networks were created as a technique of forecasting shear strength without the need for sophisticated models. Next, a multi-objective optimization problem was solved, with the goal of providing a simple design formula for evaluating the shear strength contribution supplied by a near-surface mounted system, which was the outcome of comparing the experimental findings of beams with and without NSM-FRP reinforcement. Both techniques' performances were compared to various experimental outcomes. In another study by Perera et al. using artificial intelligence, two new methods were presented for the first time as alternatives to conventional methods. Using neural networks to predict shear capacities without using complex models was one method, and genetic algorithms were another way to determine how shear mechanisms behave suitably. A comparison was made between the predictions from both approaches and the experimental results.

An externally bonded (EB) FRP concrete beam reinforced with machine learning was studied for its ultimate torsion strength by Deifalla and Salem [51]. A laboratory dataset was gathered from previous studies. The various models were described. A number of machine learning models were created and tested. The broad NN model produced the most accurate findings, with coefficients of determination, root mean square error, mean average error, an average safety factor, and coefficients of variation of 0.93, 1.66, 0.98, 1.11, and 45%, respectively.

2. Methodology

The considered method in this research starts with collecting, sorting, and statistically analyzing a database of the previous literature; then, this database is used to develop five AI-based models to predict the compressive strength of the confined concrete. Finally, the performances of these models are evaluated and discussed in terms of prediction accuracy, and the conclusions summarize the research outcomes. Figure 1 presents the formwork of this research.

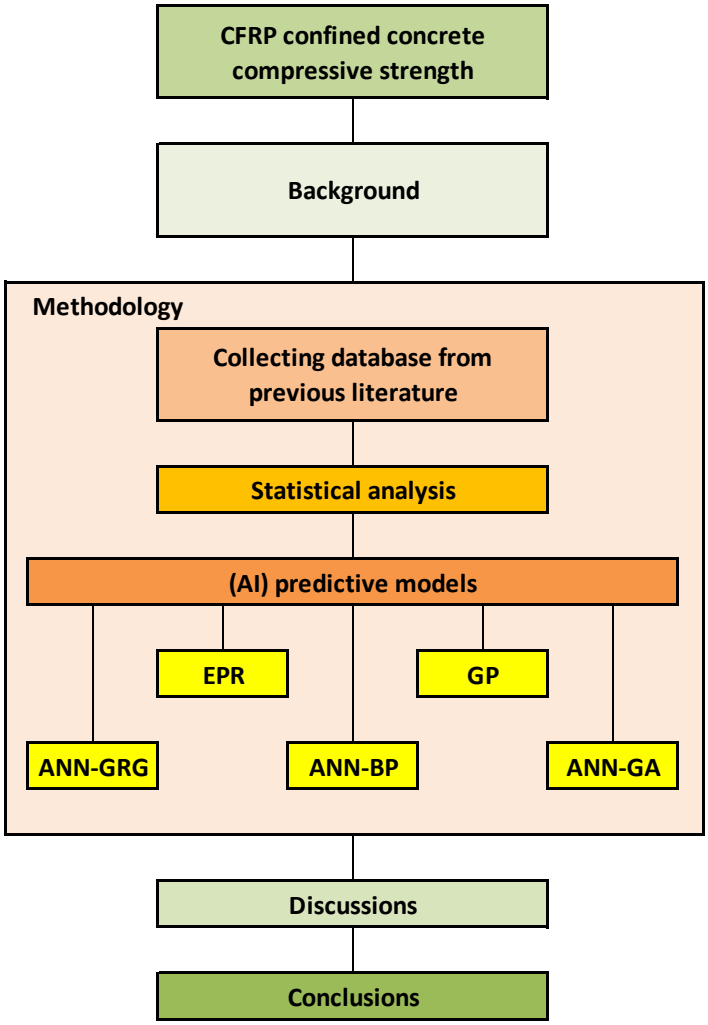

Figure 1. The formwork of the research.

2.1. CFRP Confined/Wrapped Concrete Data Collection

The databases in the research paper were collected through an extensive literature search of previously published resources relevant to this work. Previous studies [41,44,52–54] have used uniaxial compression and eccentric loading conditions to study the compressive strength of jacketed fiber-reinforced polymer concrete at different times, and the data collected from

this literature represent universal data because of its scope. The utilized dataset is listed in Appendix A.

2.2. CFRP Confined/Wrapped Concrete Data Collection

As a result of searching through previous work on the compressive capacity of CFRP-wrapped concrete columns, 164 records were collected for experimentally tested samples of axially loaded short specimens of circular columns wrapped with CFRP sheets, as presented in the Appendix A. The database includes the following fields:

- d specimen diameter (mm);
- L specimen length (mm);
- Fco compression strength of unwrapped concrete cylinder (MPa);
- t the thickness of the used CFRP sheets (mm);
- Ftf tension capacity of the used CFRP sheets (MPa);
- Ef modulus of elasticity of the used CFRP sheets (GPa);
- Fcc compression strength of wrapped concrete cylinder (MPa).

The database was split into 20% validation dataset and 80% training dataset. Tables 1 and 2 summarize their statistical characteristics and the Pearson correlation matrix, respectively. Finally, Figure 2 shows the histograms for both inputs and outputs.

From Table 3 and Figure 1, the high correlation between column diameter (d) and column length (L) can be noted. This is because all experimental tests were carried out on standard cylinder samples, (100 × 200 mm) or (150 × 300 mm), with some tolerances in the dimensions. Accordingly, one of these two factors was independent, and the other was dependent. However, due to the existing tolerances, they both were considered as independent factors in this study.

Table 1. Summary of statistical analysis results.

	d mm	**L mm**	**Fco MPa**	**t mm**	**Ftf MPa**	**Ef GPa**	**Fcc MPa**
			Training set				
Min.	100.0	200.0	18.0	0.1	365.0	19.0	36.5
Max.	300.0	610.0	63.0	5.3	4198.0	629.6	161.3
Avg.	149.5	304.3	38.3	0.7	2374.1	173.0	71.6
SD	31.3	73.4	10.4	0.7	1353.9	109.4	22.2
VAR	0.2	0.2	0.3	1.1	0.6	0.6	0.3
			Validation set				
Min.	100.0	200.0	18.0	0.1	167.0	13.0	41.3
Max.	300.0	600.0	52.2	3.0	4198.0	420.0	129.0
Avg.	153.3	307.0	35.1	0.7	2370.5	160.5	65.6
SD	28.0	56.0	7.0	0.8	1386.3	97.6	17.0
VAR	0.2	0.2	0.2	1.1	0.6	0.6	0.3

Table 2. Correlation coefficient matrix.

	d	**L**	**Fco**	**t**	**Ftf**	**Ef**	**Fcc**
d	1.00						
L	0.88	1.00					
Fco	−0.09	−0.14	1.00				
t	0.10	0.15	0.05	1.00			
Ftf	0.04	−0.04	−0.20	−0.60	1.00		
Ef	−0.12	−0.14	−0.26	−0.54	0.67	1.00	
Fcc	−0.08	−0.10	0.26	0.30	0.13	−0.01	1.00

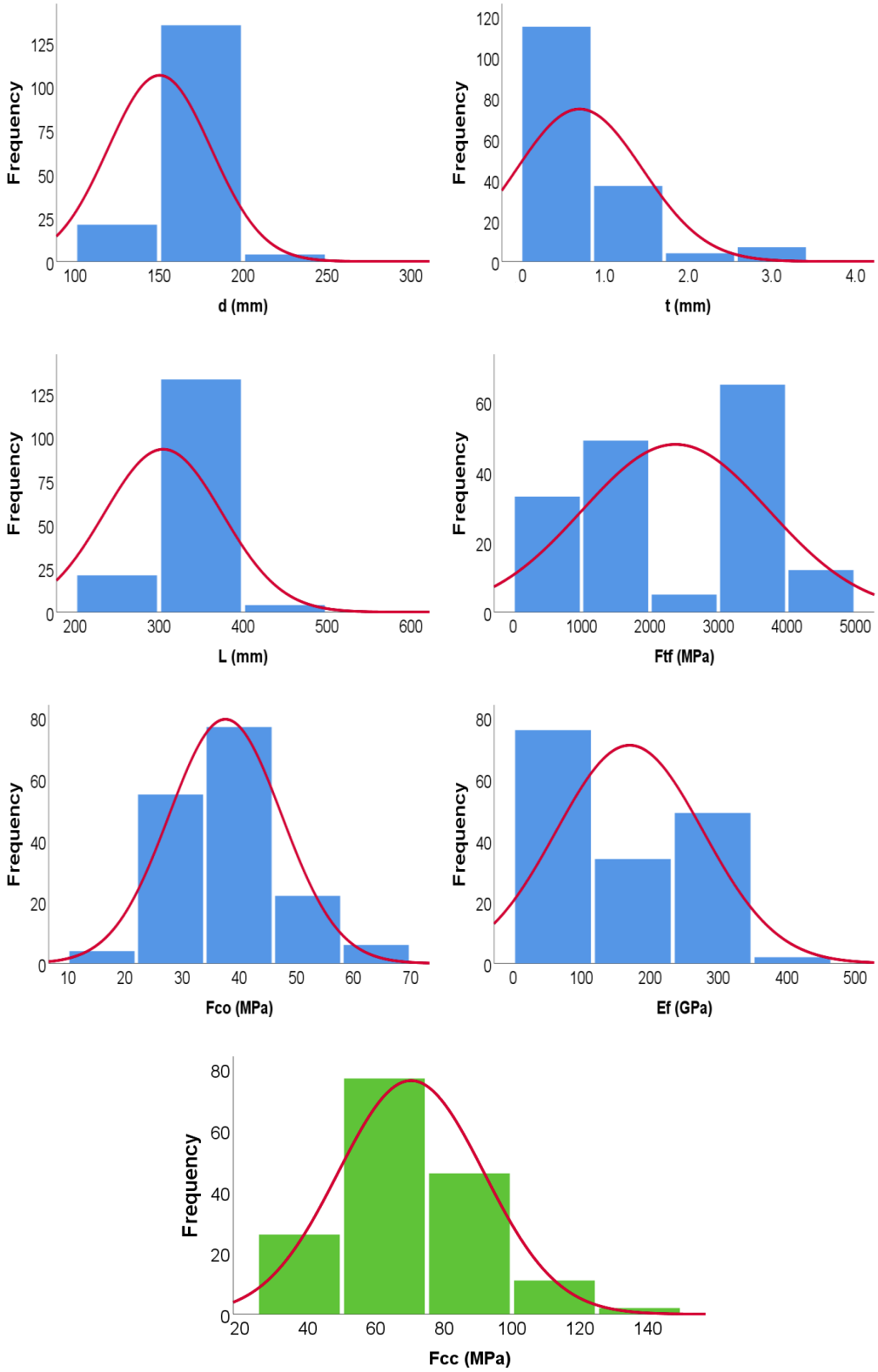

Figure 2. Variables' histograms, outputs (green), and inputs (blue).

2.3. Predictive Models

Five AI approaches were applied on the gathered records. The used techniques were "Evolutionary Polynomial Regression" (EPR), "genetic programming" (GP), and three models of the "artificial neural network" (ANN) with different training. All of the five

mentioned approaches were used to estimate the "confined cylinder compressive strength of concrete" (Fcc) in MPa, using specimen diameter (d), specimen length (L), and CFRP sheet thickness (t) in mm, in addition to the "cylinder compressive strength of unconfined concrete" (Fco) and tension capacity of CFRP sheets (Ftf) in MPa and their modulus of elasticity (Ef) in GPa.

The considered predictive techniques presented different AI approaches. Generally, ANN simulates human brain behavior, but it could be trained using a mathematical approach (BP), iterative approach (GRG), or evolutionary approach (GA). On the other hand, both GP and EPR are direct applications for the evolutionary technique (GA) [53–56]. For all the developed predictive models, the target function was the "Sum of Squared Errors" (SSE). The results of the research program in terms of prediction accuracy are discussed in the next section.

3. Results and Discussion

3.1. General Behavior of the Wrapped Concrete Column

The collected data show that the thickness of the carbon fiber-reinforced polymer (t) increases the fiber rupture strength, the elastic modulus of the CFRP, and, of course, the compressive strength of the concrete columns wrapped with CFRP. FRP layer thickness (t) and its tensile strength (Ftf) have a major impact on the Fcc value, which presents the effect of the confinement stress (t. Ftf/d) on the confined compressive strength (Fcc). This behavior is the same with equal unconfined concrete strength and dimensions, as reported by previous literature [24,38–46,52–54]. The fiber thickness influences the fiber rupture strength and the compressive strength of the wrapped concrete columns. This shows that the behavior of the CFRP-confined concrete primarily depends on two variables: the fiber polymer thickness (t) and the rupture strength of the fiber (Ftf).

3.2. Prediction of Fcc Values

3.2.1. ANN Approaches

Three ANN predictive models were developed. Each model was trained using a different technique, the first using "Back Propagation (BP)", the second using "Gradually Reduced Gradient (GRG)", and the last one using "Genetic Algorithm (GA)". The architecture of all the three networks is (6:6:1). Moreover, they all share the same activation function (Hyper Tan) and normalization method (−1.0 to 1.0).

The architecture of the networks is shown in Figure 3, and their matrixes of weights are listed in Tables 3–5. The error percentage values were 5.9%, 5.8%, and 6.4%, and the R^2 values were 0.960, 0.961, and 0.952, respectively. The importance of each parameter is presented in Figure 4; it shows that CFRP properties, the thickness of the sheets (t) and tensile strength of the wrapping sheets (Ftf), are the most important factors, while the factors of unwrapped compressive strength (Fco) and sample dimensions (d and L) have a much lower influence. The relations between the calculated and predicted values are shown in Figure 5b–d.

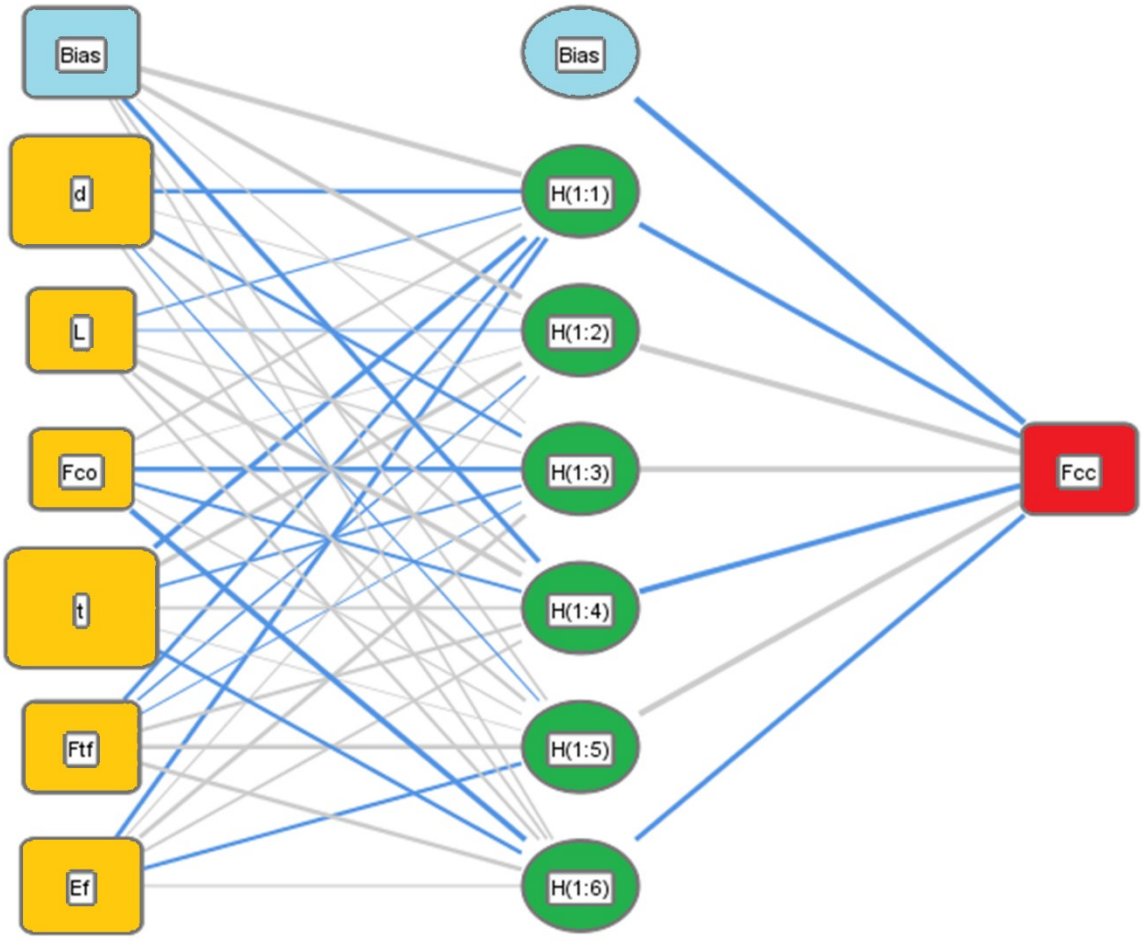

Figure 3. Architecture layout for the developed ANN models.

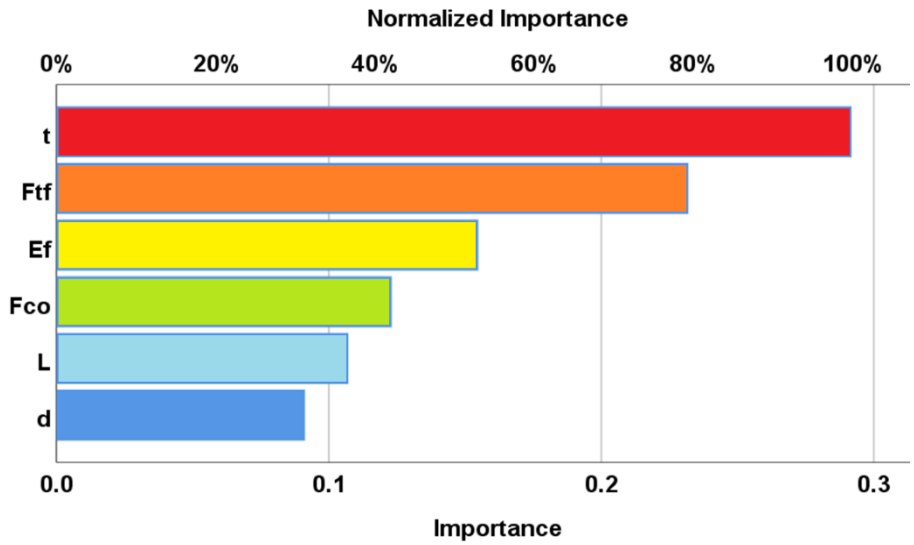

Figure 4. Relative importance of input parameters.

Table 3. Matrix of weights for ANN—BP network.

		Hidden Layer						
		H (1:1)	H (1:2)	H (1:3)	H (1:4)	H (1:5)	H (1:6)	
Input Layer	**(Bias)**	2.298	1.054	0.046	−1.003	0.171	0.160	
	d	−0.755	0.023	−0.576	0.460	−0.086	0.269	
	L	−0.119	−0.022	0.113	1.274	0.488	0.383	
	Fco	0.326	0.001	−0.969	−0.399	0.096	−1.868	
	t	−1.134	0.928	−0.270	0.308	0.009	−0.590	
	Ftf	−0.651	−0.141	−0.045	0.542	0.892	0.749	
	Ef	−0.814	0.067	0.695	0.304	−0.577	0.139	
Output		**Hidden Layer**						
		H (1:1)	H (1:2)	H (1:3)	H (1:4)	H (1:5)	H (1:6)	(Bias)
	Fcc	−1.724	3.071	1.948	−2.161	2.409	−0.987	−2.656

Table 4. Matrix of weights for ANN—GRG network.

		Hidden Layer						
		H (1:1)	H (1:2)	H (1:3)	H (1:4)	H (1:5)	H (1:6)	
Input Layer	**(Bias)**	−2.118	−0.155	1.590	0.088	3.604	−1.593	
	d	−0.325	0.173	−1.436	1.302	0.182	−0.595	
	L	−0.480	1.432	−1.026	1.526	−0.724	0.103	
	Fco	−0.267	0.058	−0.088	0.083	0.072	−1.264	
	t	1.068	−2.178	3.266	−0.191	3.324	−0.916	
	Ftf	−1.997	−0.249	0.269	−0.724	−0.156	−2.875	
	Ef	−0.484	−0.173	1.742	−0.050	−0.238	−2.793	
Output		**Hidden Layer**						
		H (1:1)	H (1:2)	H (1:3)	H (1:4)	H (1:5)	H (1:6)	(Bias)
	Fcc	−1.690	−3.748	−1.952	0.658	3.709	−0.932	−2.788

Table 5. Matrix of weights for ANN—GA network.

		Hidden Layer						
		H (1:1)	H (1:2)	H (1:3)	H (1:4)	H (1:5)	H (1:6)	
Input Layer	**(Bias)**	1.703	−3.786	−1.735	3.387	−7.024	−3.192	
	d	4.490	2.758	0.693	2.336	3.055	3.803	
	L	5.030	6.018	0.230	1.216	6.178	4.085	
	Fco	−4.781	−2.707	0.062	−5.521	−0.220	2.318	
	t	−5.914	−5.006	−14.219	−4.898	0.185	1.355	
	Ftf	0.126	3.619	0.918	−0.835	10.729	11.586	
	Ef	0.101	2.688	−1.512	0.328	−6.343	1.150	
Output		**Hidden Layer**						
		H (1:1)	H (1:2)	H (1:3)	H (1:4)	H (1:5)	H (1:6)	(Bias)
	Fcc	−3.293	−6.103	−12.682	3.349	6.661	6.336	−6.252

3.2.2. GP Approach

The used GP predictive model has four levels of complexity. The population size, survivor size, and number of generations were 75,000, 25,000, and 100 respectively. Equation (1) presents the output formula for Fcc, while Figure 5a shows the fitness. The average error % of the total dataset was (10.8%), while the R^2 value was 0.865. This implies that the closed-form equation with Fco, Ftf, and L as the dependent variables can be used to predict the Fcc at an accuracy of about 86%.

$$\text{Fcc} = \frac{2\ \text{Fco}}{3} + \frac{8\ \text{Ftf.t}}{\text{L}} + \text{Ln}(7\ \text{Ftf}) + 7 \quad (1)$$

3.2.3. EPR Approach

The last model is the EPR model; it has four levels for six input parameters, and there is a possibility for 28 terms (21 + 6 + 1 = 28), presented in a global equation, Equation (2), which is as follows:

$$\sum_{i=1}^{i=6}\sum_{j=1}^{j=6} X_i.X_j + \sum_{i=1}^{i=6} X_i + C \quad (2)$$

The evolutionary GA approach was used to select the 15 most influential terms out of the 28. The outcomes are shown in Equation (3), and the fitness is presented in Figure 5e. The error percentage and R^2 values were 7.3% and 0.939, respectively. The total results of the research program are listed in Table 6.

$$\text{Fcc} = \frac{179\ \text{L} - 187\ \text{Ftf}}{\text{d}} + \frac{377\ \text{Ftf}}{\text{L}} - \frac{123\ \text{t}^2 + 279}{\text{t.Fco}} + \frac{\text{Fco.Ftf} + 82\ \text{t.Ftf} - 66\ \text{Ftf}}{3375} + \frac{258\ \text{Fco} + 1534\ \text{t} - 15,433}{\text{Ftf}} + \frac{10,250 + \text{Ftf} - 231\ \text{Fco}}{900\ \text{t}} - 299 \quad (3)$$

Figure 6 presents the variance diagram between the measured and predicted models. The Taylor diagram in Figure 7 shows the standard deviation (compressive strength) and correlation between the predicted models and measured data, as well as the root mean square error (RMSE) envelop of the model output and the compressive capacity of the CFRP-wrapped concrete columns. The optimized compressive strengths of the proposed models in MPa are also illustrated in Figure 5, which compares them to those of the measured strength, shown as a little above 20 MPa. While all the models except GP performed within the correlation band of between 95% and 99%, they all performed within the error envelope of 5% and 10% [55–57]. Figure 6 compares the variance between the measured values and modeled values. The measured values compare best with the ANN-GRG model, with 96.1% and 5.8% performance indices, also presented in Table 6. The DFFITS plot, also known as difference in fits, which was proposed by Welsch and Kuh [58], determines the maximum number of outliers and the influential data point. It assesses the number of standard deviations that the fitted value changes when the ith information point is precluded. Figure 8 shows the DFFITS plots made based on the developed models. From the DFFITS figure, it was exposed that the developed models have few outliers, specifically the ANN-BP and EPR models, and all the plots provide the influential points among the predicted data.

Table 6. Summary of the developed models' performances.

		GP	ANN-BP	ANN-GRG	ANN-GA	EPR
MAE	Training	6.29	3.24	3.29	3.51	4.22
	Validation	5.37	3.29	2.71	3.26	3.85
RMSE	Training	7.82	4.15	4.27	4.67	5.22
	Validation	6.84	4.13	3.38	3.93	4.77
RRMSE %	Training	10.91	5.79	5.97	6.52	7.28
	Validation	10.43	6.30	5.16	5.99	7.28
MAPE%	Training	9.13	4.93	4.86	5.13	6.31
	Validation	8.27	5.04	4.27	4.94	5.97
SSE	Training	7882	2220	2356	2815	3511
	Validation	1635	596	401	540	798
Error %	Training	10.91	5.79	5.97	6.52	7.28
	Validation	10.43	6.30	5.16	5.99	7.28
R^2	Training	0.878	0.966	0.963	0.956	0.945
	Validation	0.843	0.944	0.962	0.950	0.924

MAE: Mean Absolute Error; RMSE: Root Mean Square Error; MAPE: Mean Absolute Percent Error; RRMSE: Relative Root of Mean Squared Error; SSE: Sum of Squared Errors; R^2: Coefficient of Determination.

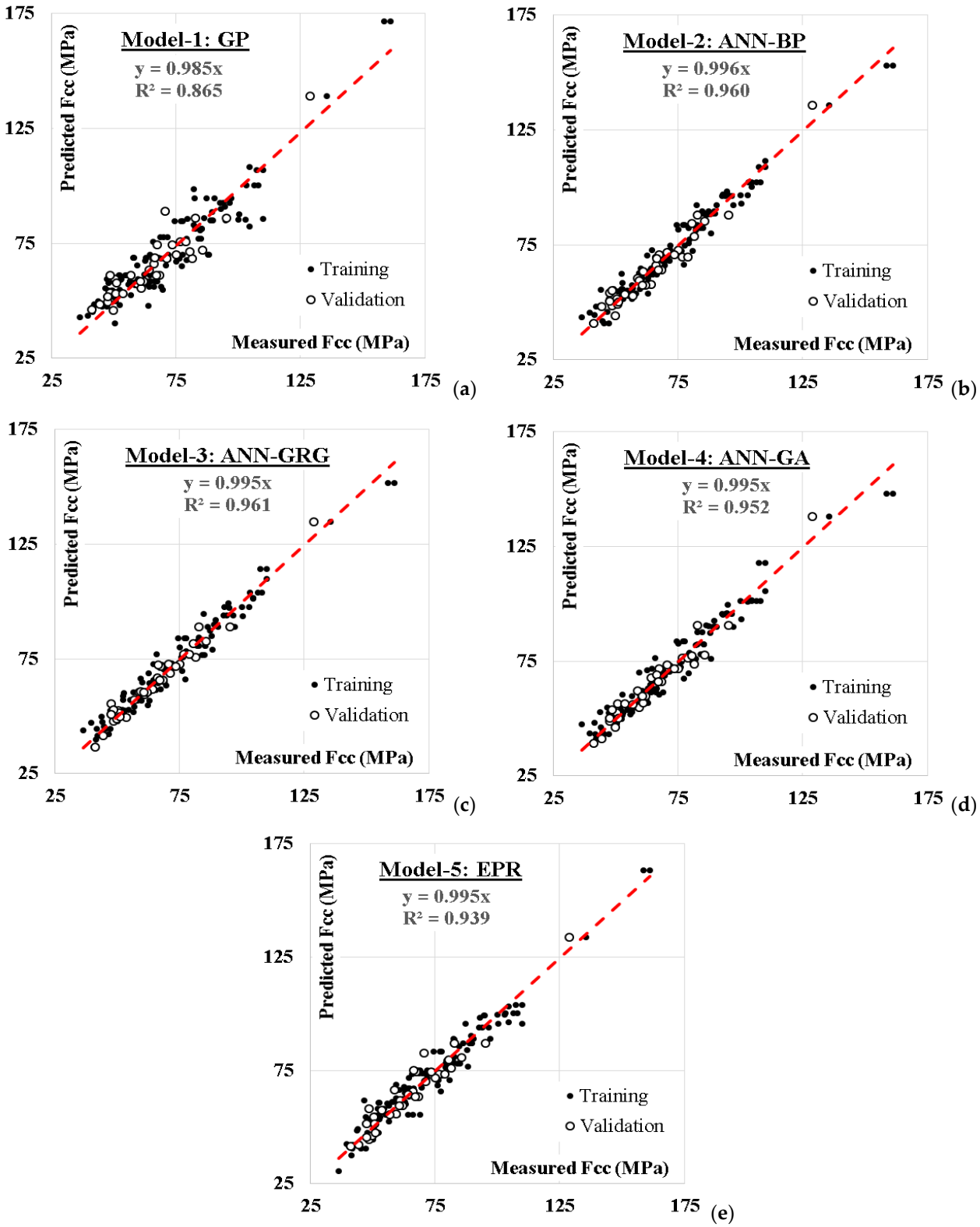

Figure 5. Relation between predicted and calculated Fcc values using the developed models. (**a**) Using GP, (**b**) using ANN-BP, (**c**) using ANN-GRG, (**d**) using ANN-GA, and (**e**) using EPR.

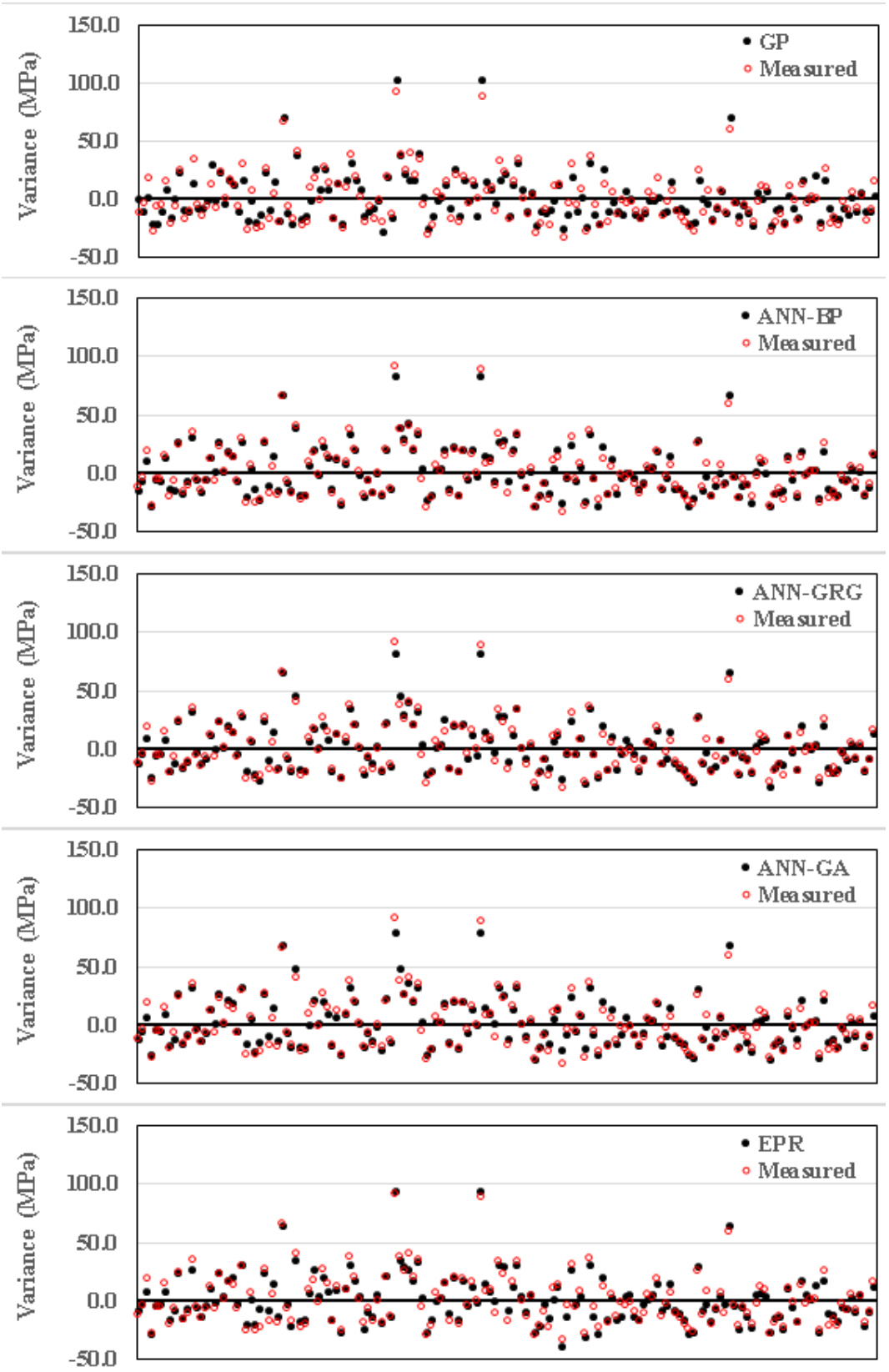

Figure 6. Variance diagram of measured and predicted models.

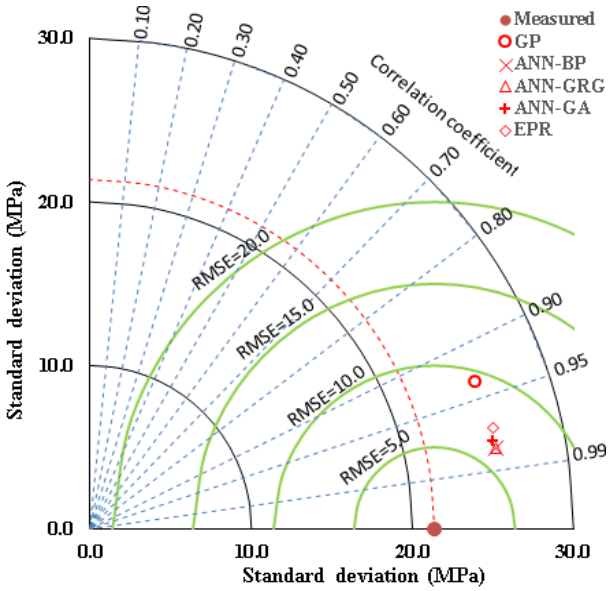

Figure 7. Taylor diagram of the predicted models.

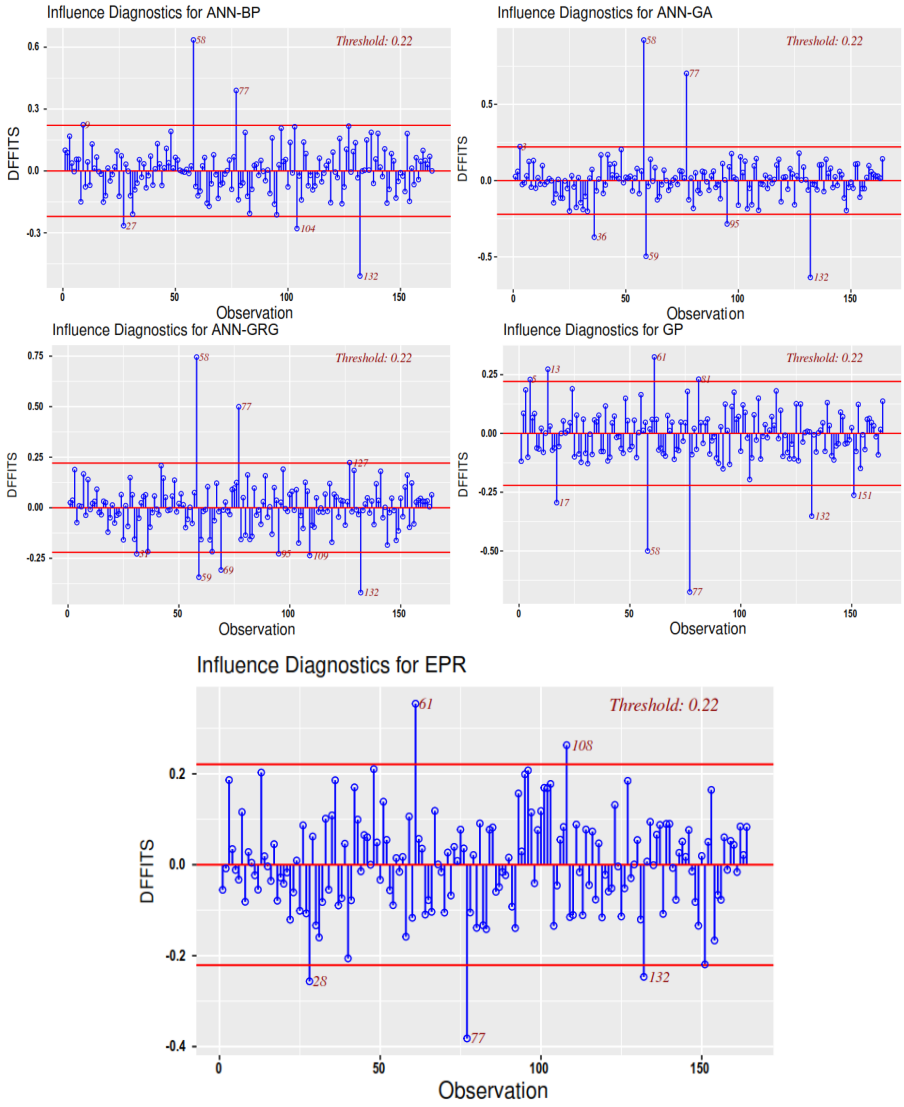

Figure 8. DFFITS plots for the predictive models.

4. Conclusions

Five predictive models for the "wrapped cylinder compressive strength of concrete (Fcc)" were presented in this study. The models were based on different AI approaches, namely "GP, ANN-BP, ANN-GRG, ANN-GA and EPR". The input parameters for all models were specimen diameter (d), specimen length (L), and thickness of CFRP sheets (t), unwrapped compressive strength (Fco), tension capacity of CFRP sheets (Ftf), and the modulus of elasticity of CFRP sheets (Ef). The outcomes of this study are:

- The GP model is the simplest but also the least accurate. Its accuracy is about 90%. The EPR model came next as a more complicated and more accurate model, with an accuracy of about 92.5%. The three ANN models presented more complicated and more accurate models with almost the same level of accuracy (94%).
- The outcomes showed that the training algorithm of the ANN model slightly affected its accuracy. Back propagation (BP) and gradually reduced gradient (GRG) showed almost the same level of accuracy, while the genetic algorithm (GA) showed a lower level of accuracy.
- Although the ANN models are more accurate than the GP and EPR models, the high complexity of the ANN models make them suitable for computerized calculations. On the other hand, the closed-form equations of GP and EPR could be used manually.
- The summation of the absolute weights of each neuron in the input layer of the developed ANN models indicates that FRP properties (t and Ftf) are the most important factors, while the factors of unwrapped compressive strength (Fco) and sample dimensions (d and L) have a much lower influence.
- The modulus of elasticity of CFRP (Ef) was not used in the GP model nor in the EPR model, which indicates its insignificant impact on Fcc compared to other parameters.
- Because the ratio (L/d) is almost constant and equals 2.0 in all the database records, these two parameters are dependent, and they both have the same importance; hence, the appearance of (L) only in the GP model is quite enough for both of them and captures the effect of size on the Fcc.
- Using the GA approach to reduce the possible 28 terms of traditional polynomial regression to only 15 terms was successful without reducing the accuracy.
- All the developed predictive models are valid within the used ranges of input parameters, and they should be verified beyond that.
- Generally, the closed-form equations proposed in this research work became decisive models in designing structural members belonging to this group of concrete columns jacketed with CFRP, with less need for the laboratory.

Author Contributions: Conceptualization, K.C.O.; methodology, A.M.E.; formal analysis, J.J. and A.S.; investigation, P.S.; data curation, R.P.S.; supervision, H.J. All authors have read and agreed to the published version of the manuscript.

Funding: This research received no external funding.

Institutional Review Board Statement: Not applicable.

Informed Consent Statement: Not applicable.

Data Availability Statement: All used data are available in the Appendix A.

Conflicts of Interest: The authors declare no conflict of interest.

Appendix A

Table A1. Utilized database.

d	L	Fco	t	Ftf	Ef	Fcc
mm	mm	Mpa	mm	Mpa	Gpa	Mpa
			Training set			
152	305	55.2	0.38	1577	105	57.9
100	200	25.9	0.167	3591	242	66.4
150	300	29.2	0.33	3788	225.7	88.2
152	305	38.6	0.31	755	73.3	41.9
152	610	26.2	2	580	87.3	64
100	200	25.9	0.167	3591	242	64.8
152	305	43.8	0.76	1577	105	85
152	305	38.6	1.22	388	27.7	49.3
152	305	55.2	0.38	1577	105	62.9
152	305	43.8	1.14	1577	105	94
152	305	35.9	0.165	4198	250.5	53.2
150	300	34.3	1	753	91	59.4
100	200	51.9	0.22	3481	230.5	104.6
152	305	38.6	0.92	822	54	64.7
152	305	41.1	0.165	3800	250.5	55.4
152	305	44.2	0.22	3762	260	62.9
152	305	18	5.31	513	35.9	82.23
160	320	61.81	1	450	34	62.68
152	305	43.8	1.14	1577	105	92.6
100	200	26.3	0.22	3481	230.5	70.9
152	305	33.7	1.14	1577	105	86.2
160	320	49.46	3	450	34	82.91
100	200	25.9	0.167	3591	242	63
150	300	52.3	0.33	3788	225.7	100
150	300	25.6	0.165	3550	235	43.9
152	305	38.6	0.92	1105	77.5	76.4
150	300	34.3	1	423	37	44.2
100	200	30.2	0.17	2716	224.6	46.6
152	305	43.8	1.14	1577	105	96.5
160	320	49.46	1	450	34	52.75
152	305	55.2	0.76	1577	105	74.6
100	200	26.3	0.11	3481	230.5	50.7
152	305	38	1.02	3615	240.7	135.7
300	600	24.5	0.501	3591	242	63
150	300	31.2	0.11	3481	230.5	52.4
152	305	38	0.68	3615	240.7	110.1
152	305	38.6	0.61	660	39.9	47.1
152	305	33.7	0.38	1577	105	49.4
150	300	45.2	0.22	3481	230.5	79.4
100	200	30.2	0.5	2873	224.6	87.2
152	305	35.9	0.33	4198	250.5	68.7
152	305	34.3	0.495	4198	250.5	97.3
152	305	43.8	0.76	1577	105	84
152	305	38.6	1.22	388	27.7	52.7
152	305	18	1.55	1353	96	82.23
152	305	38.38	0.33	795	72.4	44.87
152	305	18	2.26	978	62.5	79.49

Table A1. *Cont.*

d	L	Fco	t	Ftf	Ef	Fcc
mm	mm	Mpa	mm	Mpa	Gpa	Mpa
152	305	55.2	1.14	1577	105	108
152	305	38.6	1.22	1352	95.7	89.5
152	305	35.9	0.33	4198	250.5	71.6
152	305	37.7	0.11	3905	260	50.3
100	200	30.2	0.42	1285	576.6	63.3
152	305	41.1	0.165	3800	250.5	52.6
150	300	51.7	0.165	3788	225.7	69.2
152	610	26.2	1	580	97.1	50.6
152	305	38.38	1.32	1352	95.7	89.48
150	300	29.8	0.165	3550	235	57
152	305	38	1.36	3615	240.7	161.3
152	305	38	0.68	3615	240.7	107.4
160	320	63.01	3	450	34	94.81
100	200	33.7	0.33	3481	230.5	109.9
152	305	38.6	1.22	1352	95.7	89.9
100	200	30.2	0.67	2658	224.6	104.6
152	305	33.7	0.76	1577	105	64.6
160	320	25.93	1	450	34	39.63
152	305	33.7	0.38	1577	105	47.9
160	320	63.01	1	450	34	76.21
152	305	33.7	0.76	1577	105	71.8
100	200	26.3	0.33	3481	230.5	84.9
152	305	43.8	0.38	1577	105	52.1
152	305	34.3	0.495	4198	250.5	90.4
152	305	33.7	0.38	1577	105	49.7
152	305	38.6	1.22	1352	95.7	89
152	305	44.2	0.22	3762	260	65.7
152	305	47.6	0.33	3757	250.5	85.5
100	200	33.7	0.11	3481	230.5	69.6
152	305	38	1.36	3615	240.7	158.5
152	305	55.2	0.76	1577	105	77.6
152	305	43.8	0.76	1577	105	79.2
150	300	25.6	0.33	3550	235	59.6
150	300	52.2	0.33	3788	225.7	103
160	320	61.81	3	450	34	93.19
150	300	31.3	0.165	3788	225.7	52.3
152	305	47.6	0.33	3757	250.5	85.5
152	305	55.2	1.14	1577	105	103.3
152	305	35.9	0.33	4198	250.5	69.9
152	305	38.6	0.61	1047	70.6	56.5
100	200	42	0.6	1265	82.7	73.5
150	300	34.9	0.24	1100	420	40.7
152	305	44.2	0.11	3905	260	48.1
300	600	24.5	0.501	3591	242	60.6
152	305	35.9	0.165	4198	250.5	47.2
152	305	38.6	0.92	1105	77.5	80.9
152	305	47.6	0.33	3757	250.5	82.7

Table A1. *Cont.*

d	L	Fco	t	Ftf	Ef	Fcc
mm	mm	Mpa	mm	Mpa	Gpa	Mpa
150	300	23.6	0.11	3481	230.5	36.5
200	400	22.7	0.334	3591	242	66.3
160	320	58.24	3	450	34	100.41
100	200	25.9	0.167	3591	242	64.3
152	305	38.38	0.99	1105	77.4	77.68
100	200	30.2	0.14	1579	628.6	41.7
152	305	55.2	1.14	1577	105	106.5
200	400	22.7	0.334	3591	242	64.3
152	305	38.6	0.31	755	73.3	47.2
152	305	34.3	0.495	4198	250.5	82.6
152	305	34.3	0.165	4198	250.5	50.3
100	200	51.9	0.11	3481	230.5	75.2
152	305	34.3	0.165	4198	250.5	56.7
200	400	22.7	0.334	3591	242	69.1
152	305	38.9	0.33	3754	247	65.8
150	300	52.3	0.165	3788	225.7	68
200	400	22.7	0.334	3591	242	60.1
152	305	38.6	1.22	388	27.7	52.6
300	600	24.5	0.501	3591	242	59.4
152	305	38.6	0.92	1105	77.5	75.8
150	300	29.8	0.33	3550	235	72.1
100	200	33.7	0.22	3481	230.5	88
100	200	30.2	0.28	1824	629.6	56
150	300	31.2	0.22	3481	230.5	67.4
152	305	55.2	0.76	1577	105	77
152	305	38.38	0.66	1047	138.1	59.68
152	305	43.8	0.38	1577	105	54.7
152	305	34.3	0.165	4198	250.5	50
152	305	38.6	0.31	755	73.3	45.5
150	300	34.9	0.12	2600	200	42.2
150	300	51.7	0.33	3788	225.7	94.9
152	305	55.2	0.38	1577	105	58.1
160	320	58.24	1	450	34	77.51
152	305	38.6	0.61	660	39.9	50
150	300	34.3	2.44	365	19	62.5
Validation set						
152	305	38.9	0.33	3754	247	76.8
300	600	24.5	0.501	3591	242	58.8
152	305	38	1.02	3615	240.7	129
160	320	25.93	3	450	34	66.14
152	305	37.7	0.11	3905	260	48.5
150	300	23.6	0.33	3481	230.5	64.3
150	300	45.2	0.11	3481	230.5	59.4
160	320	29.51	1	450	34	49.88
100	200	42	0.6	1265	82.7	67.6
150	300	31.2	0.33	3481	230.5	81.7
152	305	38.9	0.33	3754	247	79.1
150	300	34.9	0.24	1100	420	41.3

Table A1. *Cont.*

d	L	Fco	t	Ftf	Ef	Fcc
mm	mm	Mpa	mm	Mpa	Gpa	Mpa
152	305	35.9	0.165	4198	250.5	50.4
152	305	41.1	0.165	3800	250.5	57
150	300	34.3	2.83	167	13	47.5
150	300	31.3	0.33	3788	225.7	80.6
152	305	38.6	0.92	822	54	68.3
150	300	23.6	0.22	3481	230.5	50.8
152	305	33.7	1.14	1577	105	82.9
150	300	52.2	0.165	3788	225.7	66.5
160	320	29.51	3	450	34	71.35
152	305	18	2.06	1127	150	70.58
150	300	34.9	0.12	2600	200	44.3
152	305	33.7	1.14	1577	105	95.4
152	305	43.8	0.38	1577	105	48.7
150	300	29.2	0.165	3788	34	53.8
152	305	38.6	0.61	660	39.9	47.7
152	305	38.6	0.92	822	54	67.3
150	300	32.2	0.165	3788	225.7	61.2
152	305	33.7	0.76	1577	105	75.2
152	305	38.6	0.61	1047	70.6	61.9
100	200	42	0.6	1265	82.7	73.5
152	305	44.2	0.11	3905	260	51.1
152	305	38.6	0.61	1047	70.6	60.6
150	300	32.2	0.33	3788	225.7	85.6

References

1. Bagheri, M.; Chahkandi, A.; Jahangir, H. Seismic Reliability Analysis of RC Frames Rehabilitated by Glass Fiber-Reinforced Polymers. *Int. J. Civ. Eng.* **2019**, *17*, 1785–1797. [CrossRef]
2. Teng, J.G.; Chen, J.-F.; Yu, T. *FRP: Strengthened RC Structures*; John Wiley & Sons, Ltd.: Hoboken, NJ, USA, 2002; Available online: https://asset-pdf.scinapse.io/prod/1824168954/1824168954.pdf (accessed on 22 May 2022).
3. Jahangir, H.; Khatibinia, M.; Kavousi, M. Application of Contourlet Transform in Damage Localization and Severity Assessment of Prestressed Concrete Slabs. *J. Soft Comput. Civ. Eng.* **2021**, *5*, 39–68. [CrossRef]
4. Prado, D.M.; Araujo, I.D.G.; Haach, V.G.; Carrazedo, R. Assessment of Shear Damaged and NSM CFRP Retrofitted Reinforced Concrete Beams Based on Modal Analysis. *Eng. Struct.* **2016**, *129*, 54–66. [CrossRef]
5. Jahangir, H.; Hasani, H.; Esfahani, M.R. Wavelet-Based Damage Localization and Severity Estimation of Experimental RC Beams Subjected to Gradual Static Bending Tests. *Structures* **2021**, *34*, 3055–3069. [CrossRef]
6. Nagender, T.; Parulekar, Y.M.; Selvam, P.; Chattopadhyay, J. Experimental Study and Numerical Simulation of Seismic Behaviour of Corroded Reinforced Concrete Frames. *Structures* **2022**, *35*, 1256–1269. [CrossRef]
7. Huang, Z.; Shen, J.; Lin, H.; Song, X.; Yao, Y. Shear Behavior of Concrete Shear Walls with CFRP Grids under Lateral Cyclic Loading. *Eng. Struct.* **2020**, *211*, 110422. [CrossRef]
8. Xu, T.; Liu, J.; Wang, X.; Guo, Y.; Chen, Y.F. Behaviour of Short CFRP-Steel Composite Tubed Reinforced Normal and High Strength Concrete Columns under Eccentric Compression. *Eng. Struct.* **2020**, *205*, 110096. [CrossRef]
9. Al-Mekhlafi, G.M.; Al-Osta, M.A.; Sharif, A.M. Behavior of Eccentrically Loaded Concrete-Filled Stainless Steel Tubular Stub Columns Confined by CFRP Composites. *Eng. Struct.* **2020**, *205*, 110113. [CrossRef]
10. Soleymani, A.; Esfahani, M.R. Effect of concrete strength and thickness of flat slab on preventing of progressive collapse caused by elimination of an internal column. *J. Struct. Constr. Eng.* **2019**, *6*, 24–40. [CrossRef]
11. Yazeed, S.-A.E.; Abdelsalam, S.A.; Abdelaziz, A.E. CFRP-Strengthened HSS Columns Subject to Eccentric Loading. *J. Compos. Constr.* **2018**, *22*, 4018025. [CrossRef]
12. Zeng, J.J.; Teng, J.G.; Lin, G.; Li, L.J. Large-Scale FRP-Confined Rectangular RC Columns with Section Curvilinearization under Axial Compression. *J. Compos. Constr.* **2021**, *25*, 4021020. [CrossRef]
13. Deng, Z.; Chai, W.; Liu, B.; Hu, Y. Compression Behavior of CFRP–Confined Coral Aggregate Concrete (CCAC) Circular Stub Columns. *Case Stud. Constr. Mater.* **2022**, *16*, e00863. [CrossRef]
14. Jahangir, H.; Esfahani, M.R. Experimental Analysis on Tensile Strengthening Properties of Steel and Glass Fiber Reinforced Inorganic Matrix Composites. *Sci. Iran.* **2020**, *28*, 1152–1166. [CrossRef]
15. Dundar, C.; Erturkmen, D.; Tokgoz, S. Studies on Carbon Fiber Polymer Confined Slender Plain and Steel Fiber Reinforced Concrete Columns. *Eng. Struct.* **2015**, *102*, 31–39. [CrossRef]

16. Gergely, I.; Pantelides, C.P.; Nuismer, R.J.; Reaveley, L.D. Bridge Pier Retrofit Using Fiber-Reinforced Plastic Composites. *J. Compos. Constr.* **1998**, *2*, 165–174. [CrossRef]
17. Bank, L.C. Progressive Failure and Ductility of FRP Composites for Construction: Review. *J. Compos. Constr.* **2013**, *17*, 406–419. [CrossRef]
18. Chotickai, P.; Tongya, P.; Jantharaksa, S. Performance of Corroded Rectangular RC Columns Strengthened with CFRP Composite under Eccentric Loading. *Constr. Build. Mater.* **2021**, *268*, 121134. [CrossRef]
19. Nematzadeh, M.; Mousavimehr, M.; Shayanfar, J.; Omidalizadeh, M. Eccentric Compressive Behavior of Steel Fiber-Reinforced RC Columns Strengthened with CFRP Wraps: Experimental Investigation and Analytical Modeling. *Eng. Struct.* **2021**, *226*, 111389. [CrossRef]
20. Naser, M.Z.; Hawileh, R.A.; Abdalla, J.A. Fiber-Reinforced Polymer Composites in Strengthening Reinforced Concrete Structures: A Critical Review. *Eng. Struct.* **2019**, *198*, 109542. [CrossRef]
21. Habil, A.; Neaz, S.M.; Hadi, M.N. Experimental Investigation on the Behavior of Hollow-Core Glass Fiber-Reinforced Concrete Columns with GFRP Bars. *J. Compos. Constr.* **2022**, *26*, 4021074. [CrossRef]
22. Al-Nimry, H.; Neqresh, M. Confinement Effects of Unidirectional CFRP Sheets on Axial and Bending Capacities of Square RC Columns. *Eng. Struct.* **2019**, *196*, 109329. [CrossRef]
23. Punurai, W.; Hsu, C.T.T.; Punurai, S.; Chen, J. Biaxially Loaded RC Slender Columns Strengthened by CFRP Composite Fabrics. *Eng. Struct.* **2013**, *46*, 311–321. [CrossRef]
24. Teng, J.G.; Lam, L. Behavior and Modeling of Fiber Reinforced Polymer-Confined Concrete. *J. Struct. Eng.* **2004**, *130*, 1713–1723. [CrossRef]
25. Abd El Fattah, A. New Axial Stress-Strain Model of Square Concrete Columns Confined with Lateral Steel and FRP. *Compos. Struct.* **2018**, *202*, 731–751. [CrossRef]
26. Harajli, M.H. Axial Stress–Strain Relationship for FRP Confined Circular and Rectangular Concrete Columns. *Cem. Concr. Compos.* **2006**, *28*, 938–948. [CrossRef]
27. Lignola, G.P.; Prota, A.; Manfredi, G.; Cosenza, E. Experimental Performance of RC Hollow Columns Confined with CFRP. *J. Compos. Constr.* **2007**, *11*, 42–49. [CrossRef]
28. Sadeghian, P.; Rahai, A.R.; Ehsani, M.R. Experimental Study of Rectangular RC Columns Strengthened with CFRP Composites under Eccentric Loading. *J. Compos. Constr.* **2010**, *14*, 443–450. [CrossRef]
29. Yang, J.; Wang, J.; Wang, Z. Rectangular High-Strength Concrete Columns Confined with Carbon Fiber-Reinforced Polymer (CFRP) under Eccentric Compression Loading. *Constr. Build. Mater.* **2018**, *193*, 604–622. [CrossRef]
30. Quiertant, M.; Clement, J.L. Behavior of RC Columns Strengthened with Different CFRP Systems under Eccentric Loading. *Constr. Build. Mater.* **2011**, *25*, 452–460. [CrossRef]
31. Pan, J.L.; Xu, T.; Hu, Z.J. Experimental Investigation of Load Carrying Capacity of the Slender Reinforced Concrete Columns Wrapped with FRP. *Constr. Build. Mater.* **2007**, *21*, 1991–1996. [CrossRef]
32. Azadeh, P.; Wei, W. Behavior of FRP Jacketed Concrete Columns under Eccentric Loading. *J. Compos. Constr.* **2001**, *5*, 146–152. [CrossRef]
33. Barros, J.A.O.; Varma, R.K.; Sena-Cruz, J.M.; Azevedo, A.F.M. Near Surface Mounted CFRP Strips for the Flexural Strengthening of RC Columns: Experimental and Numerical Research. *Eng. Struct.* **2008**, *30*, 3412–3425. [CrossRef]
34. Fitzwilliam, J.; Bisby, L.A. Slenderness Effects on Circular CFRP Confined Reinforced Concrete Columns. *J. Compos. Constr.* **2010**, *14*, 280–288. [CrossRef]
35. Hadi, M.N.S.; Le, T.D. Behaviour of Hollow Core Square Reinforced Concrete Columns Wrapped with CFRP with Different Fibre Orientations. *Constr. Build. Mater.* **2014**, *50*, 62–73. [CrossRef]
36. Chellapandian, M.; Suriya Prakash, S.; Sharma, A. Strength and Ductility of Innovative Hybrid NSM Reinforced and FRP Confined Short RC Columns under Axial Compression. *Compos. Struct.* **2017**, *176*, 205–216. [CrossRef]
37. Cao, Q.; Li, X.; Zhou, J.; Ma, Z.J. Expansive Concrete Confined by CFRP under Eccentric Compression. *Constr. Build. Mater.* **2019**, *208*, 113–124. [CrossRef]
38. Miyauchi, K.; Inoue, S.; Kuroda, T.; Kobayashi, A. Strengthening effects of concrete column with carbon fiber sheet. *Trans. Jpn. Concr. Inst.* **2000**, *21*, 143–150.
39. Karbhari, V.M.; Gao, Y. Composite Jacketed Concrete under Uniaxial Compression—Verification of Simple Design Equations. *J. Mater. Civ. Eng.* **1997**, *9*, 185–193. [CrossRef]
40. Watanabe, K.; Nakamura, R.; Honda, Y.; Toyoshima, M.; Iso, M.; Fujimaki, T.; Kaneto, M.; Shirai, N. Confinement Effect of FRP Sheet on Strength and Ductility of Concrete Cylinders under Uniaxial Compression. In Proceedings of the Third International Symposium, Sapporo, Japan, 14–16 October 1997; Volume 1, pp. 233–238.
41. Widiarsa, I.B.R. FRP-Wrapped Square RC Columns under Eccentric Loading. Ph.D. Thesis, University of Wollongong, Wollongong, Australia, 2014.
42. Rochette, P.; Labossière, P. Axial Testing of Rectangular Column Models Confined with Composites. *J. Compos. Constr.* **2000**, *4*, 129–136. [CrossRef]
43. Xiao, Y.; Wu, H. Compressive Behavior of Concrete Confined by Carbon Fiber Composite Jackets. *J. Mater. Civ. Eng.* **2000**, *12*, 139–146. [CrossRef]

44. Jiang, T.; Teng, J.G. Analysis-Oriented Stress-Strain Models for FRP-Confined Concrete. *Eng. Struct.* **2007**, *29*, 2968–2986. [CrossRef]
45. Lam, L.; Teng, J.G.; Cheung, C.H.; Xiao, Y. FRP-Confined Concrete under Axial Cyclic Compression. *Cem. Concr. Compos.* **2006**, *28*, 949–958. [CrossRef]
46. Shehata, I.A.E.M.; Carneiro, L.A.V.; Shehata, L.C.D. Strength of Short Concrete Columns Confined with CFRP Sheets. *Mater. Struct.* **2002**, *35*, 50–58. [CrossRef]
47. Nafees, A.; Javed, M.F.; Khan, S.; Nazir, K.; Farooq, F.; Aslam, F.; Musarat, M.A.; Vatin, N.I. Predictive Modeling of Mechanical Properties of Silica Fume-Based Green Concrete Using Artificial Intelligence Approaches: MLPNN, ANFIS, and GEP. *Materials* **2021**, *14*, 7531. [CrossRef] [PubMed]
48. Ahmad, A.; Farooq, F.; Niewiadomski, P.; Ostrowski, K.; Akbar, A.; Aslam, F.; Alyousef, R. Prediction of Compressive Strength of Fly Ash Based Concrete Using Individual and Ensemble Algorithm. *Materials* **2021**, *14*, 794. [CrossRef]
49. Farooq, F.; Ahmed, W.; Akbar, A.; Aslam, F.; Alyousef, R. Predictive Modeling for Sustainable High-Performance Concrete from Industrial Wastes: A Comparison and Optimization of Models Using Ensemble Learners. *J. Clean. Prod.* **2021**, *292*, 126032. [CrossRef]
50. Perera, R.; Tarazona, D.; Ruiz, A.; Martín, A. Application of Artificial Intelligence Techniques to Predict the Performance of RC Beams Shear Strengthened with NSM FRP Rods. Formulation of Design Equations. *Compos. Part B Eng.* **2014**, *66*, 162–173. [CrossRef]
51. Deifalla, A.; Salem, N.M. A Machine Learning Model for Torsion Strength of Externally Bonded FRP-Reinforced Concrete Beams. *Polymers* **2022**, *14*, 1824. [CrossRef]
52. Liang, M.; Wu, Z.-M.; Ueda, T.; Zheng, J.-J.; Akogbe, R. Experiment and Modeling on Axial Behavior of Carbon Fiber Reinforced Polymer Confined Concrete Cylinders with Different Sizes. *J. Reinf. Plast. Compos.* **2012**, *31*, 389–403. [CrossRef]
53. Bisby, L.; Ranger, M. Axial–Flexural Interaction in Circular FRP-Confined Reinforced Concrete Columns. *Constr. Build. Mater.* **2010**, *24*, 1672–1681. [CrossRef]
54. Wang, L.M.; Wu, Y.F. Effect of Corner Radius on the Performance of CFRP-Confined Square Concrete Columns: Test. *Eng. Struct.* **2008**, *30*, 493–505. [CrossRef]
55. Onyelowe, K.C.; Ebid, A.M.; Mahdi, H.A.; Soleymani, A.; Jayabalan, J.; Jahangir, H.; Samui, P.; Singh, R.P. Modeling the Confined Compressive Strength of CFRP-Jacketed Noncircular Concrete Columns Using Artificial Intelligence Techniques. *Cogent Eng.* **2022**, *9*, 2122156. [CrossRef]
56. Onyelowe, K.C.; Gnananandarao, T.; Ebid, A.M.; Mahdi, H.A.; Ghadikolaee, M.R.; Al-Ajamee, M. Evaluating the Compressive Strength of Recycled Aggregate Concrete Using Novel Artificial Neural Network. *Civ. Eng. J.* **2022**, *8*, 1679–1693. [CrossRef]
57. Ebid, A.M. 35 Years of (AI) in Geotechnical Engineering: State of the Art. *Geotech. Geol. Eng.* **2021**, *39*, 637–690. [CrossRef]
58. Welsch, R.E.; Kuh, E. *Linear Regression Diagnostics*; NBER: Cambridge, MA, USA, 1977.